Targeted Delivery of Doxorubicin by HPMA Copolymer-Hyaluronan Bioconjugates

Yi Luo,[1] Nicole J. Bernshaw,[2] Zheng-Rong Lu,[3] Jindrich Kopecek,[3] and Glenn D. Prestwich[1,2,4]

Received December 13, 2001; accepted January 4, 2002

Purpose. Overexpression of hyaluronan (HA) receptors on cancer cells results in enhanced endocytotic uptake of the drug conjugate. An *N*-(2-hydroxypropyl)methacrylamide (HPMA)-HA polymeric drug delivery system was used for targeted delivery of doxorubicin to cancer cells.

Methods. HA-doxorubicin (DOX) bioconjugates (HA-DOX), and HPMA copolymer-DOX conjugates containing HA as a side chain (HPMA-HA-DOX) were synthesized. The cytotoxicity of the polymer-drug conjugate was evaluated *via in vitro* cell culture. The internalization of the conjugate was visualized by fluorescence microscopy.

Results. Cytotoxicity of HPMA-HA-DOX targeted bioconjugate was higher against human breast cancer (HBL-100), ovarian cancer (SKOV-3), and colon cancer (HCT-116) cells when compared to the non-targeted HPMA-DOX conjugate. Fluorescence confocal microscopy revealed that the targeted HPMA-HA-DOX conjugates were internalized more efficiently by cancer cells relative to the non-targeted HPMA-DOX conjugate. Both HPMA-DOX and HPMA-HA-DOX showed minimal cytotoxicity toward mouse fibroblast NIH 3T3 cells. The internalization of polymer conjugates was correlated with their cytotoxicity.

Conclusions. Selective delivery of anti-cancer agents to cancer cells was achieved by biochemical targeting. The HA-modified HPMA copolymer showed improved toxicity due to receptor-mediated uptake of the macromolecular drug.

KEY WORDS: polymer-drug conjugates; HPMA copolymer; hyaluronan; receptor-mediated targeting; doxorubicin; cancer.

INTRODUCTION

A major challenge in cancer therapy is the selective delivery of small molecule anti-cancer agents to tumor cells. Water-soluble polymer-anti-cancer drug conjugates offer great potential and have demonstrated good aqueous solubility, increased half-life in the body, and high anti-tumor effects. Poly(styrene-*co*-maleic acid)-neocarzinostatin conjugate (SMANCS) was approved for the treatment of liver cancer in Japan (1). The conjugates of doxorubicin (DOX) to *N*-(2-hydroxypropyl)methacrylamide (HPMA) copolymers (HPMA-DOX conjugate, PK1) have passed Phase I clinical trials and are currently in Phase II trials (2). HPMA-camptothecin was also pre-clinically evaluated and is now in Phase I trials (3).

Anti-cancer polymer-drug conjugates can be divided into two targeting modalities: passive and active. The biologic activity of the passive targeting is based on the anatomic characteristics of tumor tissue, and allows polymer-drug conjugate to more easily permeate tumor tissues and accumulate over time. This is one of the principal reasons for the success of polymeric drugs, and it is often referred to as the enhanced permeability and retention (EPR) effect (1). Active targeting in drug delivery systems can be achieved by exploiting specific interactions between receptors on the cell surface and targeting moieties conjugated to the polymer backbone. The active approach therefore takes advantage of the EPR effect, but further increases the therapeutic index through receptor-mediated uptake by target cancer cells. Previous studies showed that *N*-acylated galactosamine (4) and monoclonal antibody fragments (5) were valuable targeting moieties for HPMA-DOX conjugates, selectively increasing the cytotoxicity of the polymer-drug conjugates to tumor cells.

Hyaluronic acid (HA), a linear polysaccharide of alternating D-glucuronic acid (GlcUA) and *N*-acetyl-D-glucosamine (GlcNAc) units, serves a variety of functions within the extracellular matrix (6). These include direct receptor-mediated effects on cell adhesion, growth and migration (7) and as a signaling molecule in cell motility, inflammation, wound healing, and cancer metastasis (8). These effects occur *via* intracellular signaling pathways in which HA binds to, and is internalized by, cell-surface receptors. Most malignant solid tumors and their surrounding stromal tissue contain elevated levels of HA (9), and these high levels of HA production provide a matrix that facilitates invasion (10). In addition to elevated HA in the environment surrounding tumors, most malignant cell-types overexpress the HA receptors CD44 and RHAMM. Isoforms of HA receptors, CD44 and RHAMM are overexpressed in transformed human breast epithelial cells (11), ovarian tumor cells (12), colon cancer (13), lung cancer (14), stomach cancer (15), acute leukemia (16), and other cancers (17). As a result, malignant cells with the highest metastatic potential often show enhanced binding and internalization of HA (18).

Targeting of anti-cancer agents to tumor cells and tumor metastases can be accomplished by receptor-mediated uptake of bioconjugates of anticancer agents conjugated to HA (19,20), followed by the release of free drugs through the degradation of HA in cell compartments. In this study, cell-targeted HA-DOX bioconjuagtes and HPMA copolymer-DOX conjugates containing HA as a side chain (HPMA-HA-DOX) were synthesized based on the specific interaction between HA and its receptors overexpressed on the cancer cell-surface. Selective *in vitro* cell cytotoxicity was studied using three human cancer cell lines (HCT-116 colon tumor, HBL-100 breast cancer, and SK-OV-3 ovarian cancer), and non-cancerous mouse fibroblast NIH 3T3 cells as a negative control. In addition, enhanced uptake of the HPMA-HA-DOX conjugate into cancer cells was observed relative to the non-targeted HPMA-DOX, as visualized using the intrinsic fluorescence of the DOX. This direct observation of the intracellular drug-HA conjugate provides additional evidence for the uptake of the targeted conjugates through a receptor-mediated pathway.

[1] Department of Medicinal Chemistry.
[2] Center for Cell Signaling.
[3] Department of Pharmaceutics and Pharmaceutical Chemistry, The University of Utah, Salt Lake City, Utah.
[4] To whom correspondence should be addressed. (e-mail: gprestwich@deans.pharm.utah.edu)

0724-8741/02/0400-0396/0

MATERIALS AND METHODS

Reagents

Fermentation-derived HA (sodium salt, M_r 1.5 MDa) was provided by Clear Solutions Biotech, Inc. (Stony Brook, NY, USA). 1-Ethyl-3-(3-(dimethylamino)-propyl)carbodiimide (EDCI), adipic dihydrazide (ADH), succinic anhydride, anhydrous DMF, and triethylamine were purchased from Aldrich Chemical Co. (Milwaukee, WI, USA). Testicular hyaluronidase (HAse), Dulbecco's phosphate-buffered saline (DPBS), 3-[4,5-dimethylthiazol-2-yl]-2,5-diphenyltetrazolium bromide (MTT), dimethyl sulfoxide (DMSO) and cell culture media were purchased from Sigma (St. Louis, MO, USA). DOX was a generous gift from Dr. A. Suarato, Pharmacia-Upjohn, Milano, Italy. Fluorescence images were recorded on a Bio-Rad (Hercules, CA, USA) MRC 1024 laser scanning confocal imaging system based on a Zeiss (Oberkochen, Germany) Axioplan microscope and a krypton/argon laser.

Cell Lines

HBL-100, a human breast cancer cell line, was maintained in culture in high glucose D-MEM (Dulbecco's Modified Eagle Medium), which was supplemented with 10% γ-irradiated fetal bovine serum (FBS) and 1% sodium pyruvate; SK-OV-3, a human ovarian cancer cell line, was cultured in D-MEM/F12 + 10% FBS; HCT-116, a colon tumor cell line, was maintained in culture in α-MEM (Minimal Essential Medium, Eagle) + 10% FBS; NIH 3T3, a mouse fibroblast noncancerous cell line, was maintained in high glucose D-MEM + 10% FBS.

Analytical Instrumentation

All ^{1}H NMR spectral data were obtained using an NR-200 FT-NMR spectrometer at 200 MHz (IBM Instruments Inc.). UV-Vis spectra were recorded on a Hewlett Packard 8453 UV-Vis diode array spectrophotometer (Palo Alto, CA, USA). HA was characterized by gel permeation chromatography (GPC) using the following system: Waters 515 HPLC pump, Waters 410 differential refractometer, and Waters™ 486 tunable absorbance detector. Waters Ultrahydrogel 250 and 2000 columns (7.8 mm ID × 30 cm) (Milford, MA, USA) were used for GPC analysis, the eluent was 150 mM pH 6.5 phosphate buffer/MeOH = 80:20 (v/v), and the flow rate was 0.5 ml/min. The system was calibrated with HA standards supplied by Dr. O. Wik (Pharmacia). HPMA copolymer conjugates were characterized by GPC on a Pharmacia FPLC with Superose analytical column, pH 7.4 phosphate-buffered saline (PBS) buffer was used as eluent with a flow rate of 0.4 ml/min. Cell viability in cell culture was determined using thiazoyl blue (MTT) protocols and measured at 540 mm (21,22) and a BIO-RAD M-450 microplate reader (Hercules, CA, USA). Laser scanning confocal microscopy was carried out on a Keller-type Bio-Rad MRC 1024 with LASERSHARP acquisition software. Fluorescence images were taken using FITC settings with the 488 nm excitation line and a 522 nm 32 bandpass filter was used to collect the images.

Preparation of Low Molecular Weight (LMW) HA and HA Adipic Dihydrazide Derivative (HA-ADH)

LMW HA was obtained by the degradation of high molecular weight HA (1.5 MDa) in pH 6.5 PBS buffer (4 mg/ml) with HAse (10 U/mg HA), and purified by dialysis against H_2O. Next, HA-ADH was prepared using a modified purification method that gives preparations free of small molecules (20). In a representative example, LMW HA (50 mg) was dissolved in H_2O to give a concentration of 4 mg/ml, and then a fivefold excess of ADH was added into the solution. The pH was adjusted to 4.75 by addition of 0.1 N HCl. Next, 2 equiv. of EDCI was added in solid form and the pH was maintained at 4.75 by addition of 0.1 N HCl. The reaction was quenched by addition of 0.1 N NaOH to adjust the pH to 7.0 for different reaction times (see below). The reaction mixture was then transferred to pretreated dialysis tubing (Mw cutoff 3,500) and dialyzed exhaustively against 100 mM NaCl, then 25% EtOH/H_2O, and finally H_2O. The purity of HA-ADH was monitored by GPC. The purified polymer solution was then filtered through 0.2 μm cellulose acetate membrane, flash frozen, and lyophilized. The loading of ADH on the polymer backbone was determined by ^{1}H NMR in D_2O (20). HA-ADH (37 mg) was obtained with 9 mol% and 18 mol% loading, based on available carboxylates modified, by using reaction times of 12 min and 20 min, respectively.

Preparation of HA-DOX Conjugates (Figure 1)

First, DOX was converted to an active ester form (DOX-NHS) (23). Thus, 20 mg DOX (34 μmol) was dissolved in 1.2 ml of anhydrous DMF, followed by addition of 15 μl triethyl-

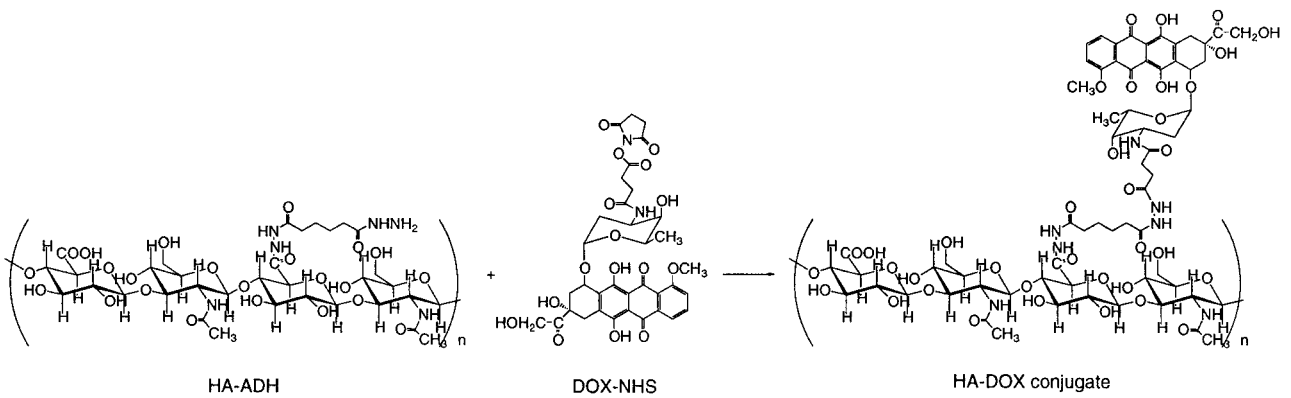

Fig. 1. Synthesis of HA-DOX conjugates.

amine and 3.8 mg succinic anhydride. The reaction was stirred at room temperature (rt) in the dark for 24 h. DOX-hemisuccinate was purified by C_{18} cartridge (Varian, Harbor City, CA), with methanol as the eluent.

Next, *N*-hydroxysuccinimido diphenyl phosphate (SDPP) was prepared from 10 mmol of diphenylphosphoryl chloride, 10 mmol of *N*-hydroxysuccinimide, and 10 mmol triethylamine in 6 ml of CH_2Cl_2 as previously described (20,24). Crude SDPP was triturated with ether, dissolved in ethyl acetate, washed (2 × 10 ml H_2O), dried ($MgSO_4$), and concentrated *in vacuo* to give SDPP with m.p. 89–90°C (85%). To the solution of DOX-hemisuccinate and 18.5 mg (1.5 equiv.) of SDPP in 2 ml DMF, was added with 60 μl (10 equiv.) triethylamine. The reaction was stirred for 6 h at rt, and then concentrated *in vacuo*. The DOX-NHS ester was purified on a LH-20 column with methanol as the eluent.

HA-DOX conjugates were prepared by the coupling of LMW HA-ADH and DOX-NHS. HA-ADH (50 mg, 9 mol%, and 18 mol%) was dissolved in 7 ml of a 3 mM phosphate buffer, pH 6.0, and then 2 mg DOX-NHS in 15 ml DMF was added to this solution in an ice-water bath. The reaction was stirred at rt for 3 days. The HA-DOX conjugates were purified on a Sephadex G-25 column using PBS buffer as the eluent, followed by dialysis against H_2O to remove the buffer salt. The DOX loading was determined by the absorption of UV spectrum at $\lambda = 484$ nm.

Preparation of HPMA-HA-DOX Conjugates (Figure 2)

The HPMA copolymer-bound DOX (HPMA-DOX) was synthesized as described (25,26). A lysosomally degradable glycylphenylalanylleucylglycine (GFLG) spacer was used as the oligopeptide side chain. The conjugate was synthesized using a two-step procedure (27). In the first step, the polymer precursor HPMA-(GFLG)-ONp was prepared by radical precipitation copolymerization of HPMA and *N*-methacryloylglycylphenylalanylleucylglycine *p*-nitrophenyl ester (26). The polymer precursor contained 7.1 mol% active ester groups (M_w = 17,800, M_n = 14,500). DOX was bound to the polymer precursor by aminolysis (28). HPMA-(GFLG)-ONp (200 mg) and DOX (21.9 mg) hydrochloride were dissolved in 1.0 ml DMSO, and 50 μl of Et_3N was then added. The mixture was stirred at rt for 1 h, and precipitated in acetone/ether (3:1). The red polymer solid was collected and washed with acetone/ether, and dried under vacuum to give 210 mg of product. The HPMA-(GFLG)-DOX-ONp conjugate contained 1.1 mol% of DOX.

HPMA-HA-DOX conjugates were prepared by the reaction of HA-ADH (9 mol% and 18 mol% hydrazide modification) with the activated ester HPMA-(GFLG)-DOX-ONp. Thus, 90 mg of HPMA-(GFLG)-DOX-ONp copolymer-drug conjugate prepared previously was dissolved in 2.0 ml DMSO, and 90 mg HA-ADH (18 mol% hydrazide modification) was dissolved in 1.0 ml H_2O and 2.0 ml DMSO. The two solutions were combined and stirred overnight at rt. Aminoethanol (100 μl) was added to destroy unreacted active ester. The HPMA-HA-DOX conjugate was isolated and purified by gel filtration on a Sephadex LH-20 column (2×), with methanol as eluent. The solvent was removed under vacuum, and the residue was dissolved in distilled H_2O and lyophilized. The DOX loading was determined by the absorption of UV spectrum at $\lambda = 484$ nm. HA composition was calculated by mass balance.

In Vitro Cell Culture

The cytotoxicity of HA-DOX and HPMA-HA-DOX reaction against HBL-100, SKOV-3, and HCT-116 cells was

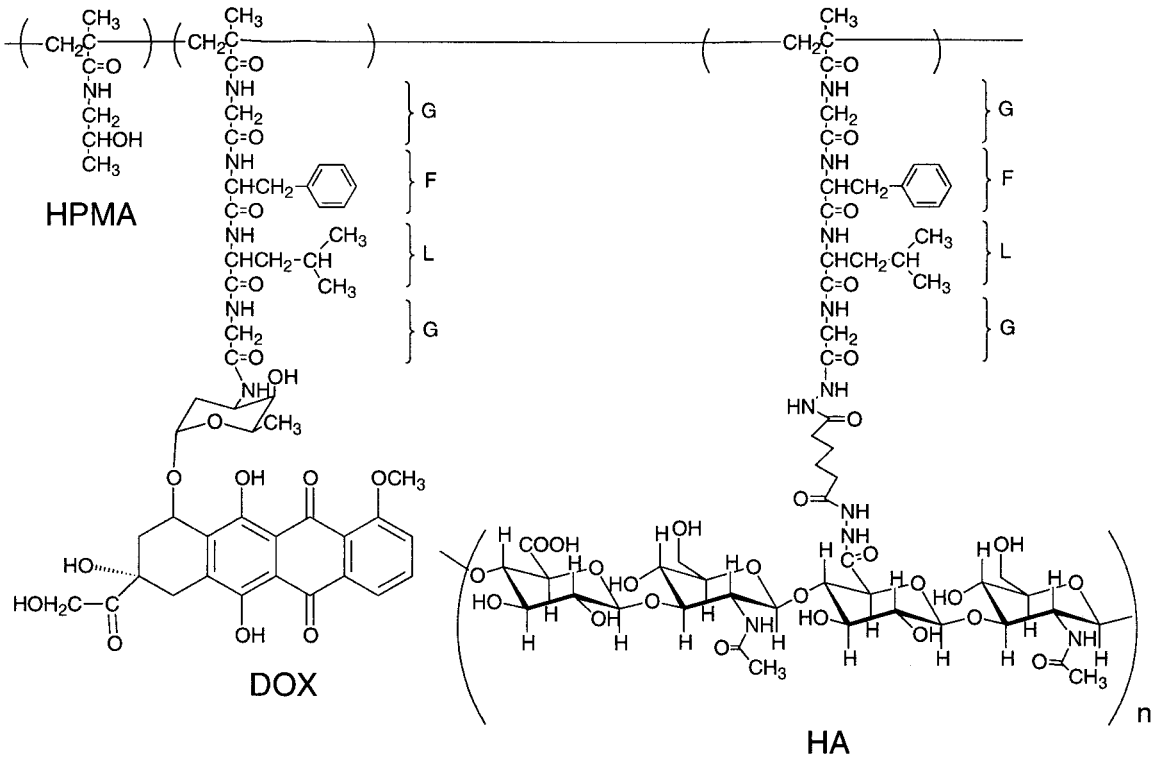

Fig. 2. Structure of HPMA-HA-DOX conjugates.

determined using a 96-well plate format in quadruplicate with increasing doses ranging from 0.001–10 mg/ml of DOX equivalent. Each well contained approximately 20,000 cells in 200 μl cell culture media. Thus, a 2-μl aliquot of the stock solution was added to each well, and cells were continuously incubated at 37 °C, 5% CO_2 for 3 days with the test substance. Next, the media was removed by aspiration and the cells were supplied with 100 μl McCoy's medium; the number of cells remaining after aspiration can be quantified by treatment with MTT. Thus, 11 μl MTT solution (5 mg/ml MTT in PBS) was added into cell culture and incubated for 4 h. Living cells metabolize MTT to a dark formazan dye. The cell culture media was removed by aspiration, and cells were washed with 3 × 100 μl DPBS buffer. Next, 100 μl DMSO was added, the suspension was gently mixed for 5 min, and the plate was read in a Biorad plate reader at 540 nm. The absorbance value provides a direct measure of the number of live cells post-treatment with the drug conjugates (21). Response was graded as percent live cells compared to untreated controls (22). Dose-response curves were constructed, and the concentration necessary to inhibit the growth of the cells by 50% relative to the non-treated control cells (IC_{50} dose) was determined.

Internalization of HPMA-HA-DOX and HPMA-DOX Conjugates by Cancer Cells

SKOV-3 cells were incubated in a cell culture flask, harvested by trypsinization, and transferred into an eight-well cell culture slide. Then, 20,000 cells were seeded in each well of the slide and cultured for 48 h. The cultured medium was replaced with medium containing HPMA-HA-DOX conjugates, and the concentration was adjusted to 50 μg/ml of HA equivalent. Meanwhile, the HPMA-DOX conjugate with an equal amount of DOX drug to HPMA-HA-DOX was used as a control. Cells were cultured with the conjugates at various time intervals. Unbound conjugate was removed by washing the cell layer 3 × with DPBS. Cells were fixed with 3% paraformaldehyde for 10 min at rt and washed again with DPBS. The internalized HPMA-HA-DOX conjugate was visualized by fluorescence confocal microscopy.

Fluorescence Microscopy

Cells were examined using an inverted microscope (Nikon) and a Bio-Rad (Hercules, CA, USA) MRC 1024 laser scanning confocal microscope. Cell images were collected by a 60 × oil immersion objective; no post-acquisition enhancement of images was performed. DOX fluorescence image acquisition was accumulated *via* the BHS block of filters: excitation 488 nm and emission through a 522 nm (32 bandpass) filter. A coverslip was mounted on a slide containing fixed cells with ProLong Antifade Kit (Molecular Probes, Eugene, OR, USA) as the mounting medium.

RESULTS AND DISCUSSION

Preparation of HA-DOX Conjugates

The hydrazide method for the preparation of HA-ADH derivatives (20) allows attachment of reporter molecules, drugs, crosslinkers, and combinations of these moieties to HA (6). The LMW HA was prepared by partial degradation of 1.5 MDa HA with testicular HAse in pH 6.5 PBS buffer at 37°C. The final size of LMW HA was characterized by GPC analysis: M_n = 3,880, M_w = 11,200, and molecular dispersity (DP) = 2.9. Next, HA-ADH derivatives with different ADH loadings were prepared by carbodiimide coupling chemistry (20), in which the extent of ADH modification was controlled through use of specific molar ratios of hydrazide, carboxylate equivalents, and carbodiimide. The purity and molecular size distribution of the HA-ADH were measured by GPC. HA-ADH with ADH loadings of 9 mol% and 18 mol% were obtained and used in the preparation of the HA-DOX and HPMA-HA-DOX conjugates.

Furthermore, HA-DOX conjugates were synthesized by the conjugation of HA-ADH to the active ester DOX-NHS to give a non-cleavable hydrazide linkage between the DOX drug and the HA polymer carrier. The DOX loading was determined by the UV spectrum at λ = 484 nm. The DOX composition of the HA-DOX conjugates used in the *in vitro* cytotoxicity test were 2.3 wt% and 3.5 wt%, which were made from 9 mol% and 18 mol% ADH loading of HA-ADH, respectively.

Preparation of HPMA-HA-DOX Conjugates

The cell-targeted delivery system was designed with HA on the side chain of the HPMA copolymer serving as a targeting moiety to the cancer cell-surface, and DOX linked to the polymer carrier through a lysosomal enzyme degradable peptide linkage (26). Thus, the designed conjugates will (**i**) increase their specificity and selectivity against cancer cells by internalization through receptor-mediated endocytosis, (**ii**) release the free active DOX drug in the lysosomal compartment following the endocytosis, (**iii**) diffuse into nucleus through cytoplasma, and (**iv**) destroy the cancer cells. HPMA-HA-DOX conjugates were synthesized by the conjugation of HA-ADH with HPMA-DOX copolymer containing an active ester (drug-polymer precursor, HPMA-(GFLG)-DOX-ONp). Two levels of modification by HA-ADH, 9 mol% and 18 mol%, were used in the conjugation. HA loading was determined by mass balance, while the DOX loading was determined by the UV absorbance at λ = 484 nm. HPMA-HA-DOX conjugates made from 18 mol% HA-ADH gave 36 wt% HA and 3.3 wt% DOX with M_w = 35,000 and M_n = 19,000. HPMA-HA-DOX conjugates made from 9 mol% HA-ADH gave 17 wt% HA and 3.2 wt% DOX with M_w = 18,000 and M_n = 14,000.

Cytotoxicity Assay of HA-DOX and HPMA-HA-DOX Conjugates

Free DOX drug, non-targeted HPMA-DOX and targeted HA-DOX, and HPMA-HA-DOX conjugates were assessed for their dose-dependent growth inhibitory effect on human breast cancer (HBL-100), ovarian cancer (SKOV-3), and colon cancer (HCT-116) cells. Each of these cell-types has been reported to overexpress HA receptors on the tumor cell-surface. The non-cancerous mouse fibroblast cell line NIH3T3 was used as a negative control. Cells were exposed to various DOX concentrations (DOX equivalent for polymer-drug conjugates) to determine the concentration necessary to inhibit the tumor cell growth by 50% relative to non-treated control cells (IC_{50} dose). Each IC_{50} value was analyzed by

polynomial curve fitting of cell viability (%) *vs.* DOX equivalent concentration.

Figure 3 more clearly illustrates dose-dependence of cell viability on the concentration of logarithm scale of DOX equivalents covalently bound to the polymer conjugates, indicating the significant cytotoxicity increase with the targeting moiety presented in the polymer-drug conjugates. The IC_{50} doses for the free DOX drug and the conjugates are summarized in Table I. From these results, it is evident that covalent attachment of DOX to a non-targeted polymer carrier (HPMA-DOX) markedly decreases the cytotoxicity of the parent drug. For SKOV-3 cells, the IC_{50} dose increases from 0.92 μM for free DOX drug to 58.2 μM for HPMA-DOX. These increases, in each of the three cancer cell lines tested, likely reflect the different mechanisms of cell uptake, e.g., free diffusion for free DOX drug *vs.* endocytosis for DOX-polymer conjugates, resulting in different intracellular drug concentration. Importantly, the targeted HPMA-HA-DOX conjugates that can enter cells by receptor-mediated endocytosis have dramatically lower IC_{50} values based on equivalent amounts of the DOX drug. The IC_{50} values against HBL-100 cells were at doses of 0.52 μM and 1.67 μM for the targeted HPMA-HA-DOX conjugates with 36 wt% and 17 wt% HA loading, respectively, in comparison to 18.7 μM for the non-targeted HPMA-DOX conjugate and 0.15 μM for free DOX drug. The cytotoxicity of targeted HPMA-HA-DOX conjugates to cancer cells showed an order of magnitude greater potency relative to HPMA-DOX. We conclude that receptor-mediated endocytosis contributed substantially to the increased cytotoxicity of the targeted conjugates. Despite the increased cytotoxicity to cancer cells, the HPMA-DOX and HPMA-HA-DOX showed minimal toxicity to normal fibroblasts.

Interestingly, the cytotoxicity of the HA-DOX conjugates was slightly lower than the non-targeted HPMA-DOX conjugate. The higher IC_{50} values against HBL-100 cells were 100 μM and 75.5 μM for HA-DOX conjugates, compared to 18.7 μM for non-targeted HPMA-DOX conjugate, and 0.52 μM for targeted HPMA-HA-DOX conjugate (36 wt%). The reduction in cytotoxicity is best explained by the poorly hydrolyzable hydrazide linkage between DOX and the HA polymer carrier. In earlier work, we showed that the cytotoxicity of HA-Taxol conjugates required an esterase-cleavable linkage (29) between Taxol and the HA polymer carrier, giving a comparable value to free Taxol drug in cell culture against HBL-100 cells (20). The lysosomal membrane has limited permeability to macromolecules, and unless the active drug is released in free form from the polymer carrier and diffuses into cytosol and nuclei, the polymer-drug conjugate remains sequestered in the lysosomal compartment (30,31). In the present example, the effectively non-cleavable linkage between DOX drug and HA carrier apparently prevents the drug from exerting its effect. The mechanism of this toxicity reduction was not further investigated.

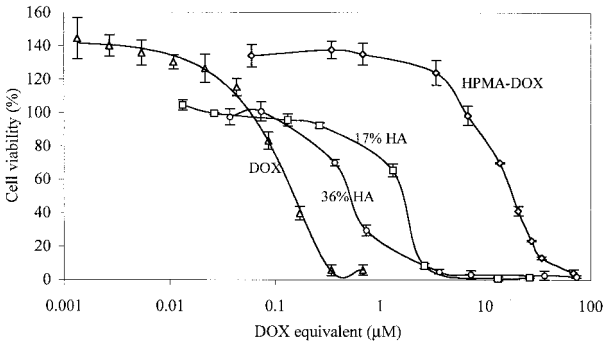

Fig. 3. *In vitro* cytotoxicity of HPMA-HA-DOX conjugates against HBL-100 human breast cancer cells, (△), free DOX drug; (◇), non-targeted HPMA-DOX conjugate; (○), targeted HPMA-HA-DOX conjugate (36 wt% HA); (□), targeted HPMA-HA-DOX conjugate (17 wt% HA). Cell viability of HBL-100 cells as function of DOX equivalent concentration. The cytotoxicity of polymer conjugates (targeted and non-targeted) were determined using the MTT assay.

With a noncancerous cell line, mouse-fibroblast NIH 3T3 as the negative control (20), the IC_{50} values of the targeted conjugates, HA-DOX and HPMA-HA-DOX were significantly higher, indicating much lower cytotoxicity (Table I). For example, the IC_{50} value of HA-DOX (3.5 wt% DOX) against HBL-100 cells was a dose of 75.5 μM; however, it was >883 μM against NIH 3T3 cells; for HPMA-HA-DOX conjugates (36 wt% HA), the IC_{50} was 0.52 μM against HBL-100 cells, but 21.2 μM against NIH 3T3 cells. This result is consistent with the selective cytotoxicity observed for HA-Taxol conjugates against cancer cells overexpressing HA receptors (20). Unlike the poorly hydrolyzable hydrazide linkage in HA-DOX conjugate, the HA-Taxol adduct used previously has an esterase-labile bond and thus free active drug was readily released inside the targeted cells. The cytotoxicity of the targeted conjugates against the control fibroblast cells was over an order of magnitude lower than for cancer cells, providing further support for the role of receptor targeting in selective uptake of the HA-containing conjugates.

Cell Binding and Uptake of HPMA-HA-DOX Conjugates

To correlate the receptor-mediated endocytosis of conjugates by cells with their cytotoxicity, the cell binding and uptake of the targeted HPMA-HA-DOX conjugates were followed by fluorescence microscopy using the intrinsic fluorescence of DOX. SKOV-3 cells were incubated with the HPMA-HA-DOX conjugates (36 wt% and 17 wt% HA loading) of 50 μg/ml HA equivalent for a range of time intervals, the non-targeted HPMA-DOX of an equal amount of DOX equivalent was used as a control. After fixing and washing, the amount of material internalized was visualized by fluorescence confocal microscopy. Cells were sectioned optically using confocal microscopy, and fluorescence images were taken *via* the BHS block of filters of excitation 488 nm and emission 522 nm.

Confocal fluorescence images of HPMA-HA-DOX uptake by SKOV-3 cells are presented in Fig. 4. Initially, the 2 h images of HPMA-HA-DOX polymer conjugates showed membrane localization. Over the course of 8 h, the HPMA-HA-DOX was gradually taken up into the cells; in 24 h, cells showed the polymer conjugates in most subcellular compartments. The uptake of HPMA-HA-DOX conjugate with 36 wt% HA loading was faster than the conjugate with 17 wt% HA loading; however, no significant difference was observed. The conjugate with higher percentage HA loading is likely binding to more cell-surface HA receptors and is thus internalized more readily. In non-targeted HPMA-DOX controls, the fluorescence uptake slowly increased with incubation time; however, very weak fluorescence (polymer conjugate

Table I. Cytotoxicity of Free DOX Drug, HA-DOX Conjugates, and HPMA-HA-DOX Conjugates against Cancer Cells (HBL-100, SKOV-3 and HCT-116) and Fibroblast NIH 3T3 Cells *in Vitro*

Drugs	IC_{50} (μM) of DOX equivalent			
	HBL-100	SK-OV-3	HCT-116	NIH 3T3
DOX	0.15	0.92	0.35	>0.68
HA-DOX (2.3 wt% DOX)	100	157	140	n.t.[a]
HA-DOX (3.5 wt% DOX)	75.5	141	62.0	>883
HPMA-DOX	18.7	58.2	56.6	>70
HPMA-HA-DOX (36 wt% HA)	0.52	9.2	4.32	21.2
HPMA-HA-DOX (17 wt% HA)	1.67	10.3	5.66	26.6

[a] n.t. = not tested.

internalization) was observed even after 24 h incubation, in comparison to the targeted HPMA-HA-DOX system. The uptake of HPMA-HA-DOX into HBL-100 cells and HCT-116 cells occurred with a similar appearance and time course.

These images provide a particularly dramatic illustration of the initial binding of the targeted HPMA-HA-DOX conjugates onto the tumor cell-surface, following rapid endocytosis *via* HA receptor-mediated pathways. HA, which has been incorporated into HPMA-DOX conjugates, significantly increases the efficiency of endocytosis by cancer cells. The cellular binding and uptake of HPMA-HA-DOX conjugates observed by confocal fluorescence images is consistent with the cytotoxicity results, and provided further support for the increased cytotoxicity of targeted HPMA-HA-DOX conjugates. We conclude that the internalization of the polymer conjugates is directly correlated to the cytotoxicity of each drug conjugate.

In summary, the data reported herein indicate that the cytotoxicity of targeted HPMA-HA-DOX polymer conjugates requires cellular uptake of the bioconjugate followed by the release of the active free DOX drug by the lysosomal enzymatic cleavage of the GFLG tetrapeptide spacer. Targeting a variety of anti-cancer agents to tumor cells and tumor metastases can be achieved by receptor-mediated uptake of an HA containing-anti-cancer agent conjugate, followed by the intracellular release of the active drug and subsequent cell death. The ability to "seek and destroy" micrometastases is one of the most compelling and attractive potential outcomes for the HA-modified macromolecular produgs.

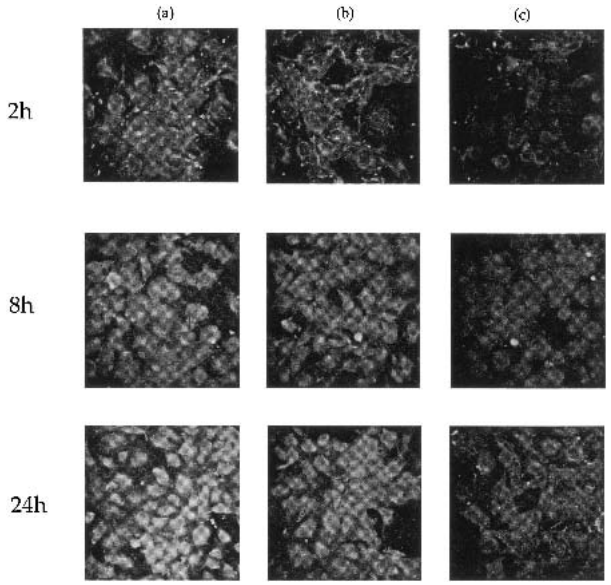

Fig. 4. Time course of bioconjugate internalization into human ovarian cancer SK-OV-3 cells: (**a**) HPMA-HA-DOX, 36 wt% HA; (**b**) HPMA-HA-DOX, 17 wt% HA; (**c**) nontargeted HPMA-DOX. Cells were incubated for 2, 8, and 24 h, respectively.

ACKNOWLEDGMENTS

Financial support for this work was provided by Department of Army (DAMD 17-9A-1-8254) to G.D.P. and by the Huntsman Cancer Foundation at The University of Utah (UUtah). J. K. acknowledges support by NIH grant CA51578. We are grateful to Joseph C. Shope and Dr. Daryll B. DeWald of Department of Biology of Utah State University for assistance with confocal microscopy. We thank Dr. L. Y.-W. Bourguignon of University of Miami Medical School for providing HBL-100 and SK-OV-3 cells. We are grateful to Clear Solutions Biotechnology, Inc. (Stony Brook, NY) for providing HA and the Center for Cell Signaling (UUtah) for access to its equipment and facilities.

REFERENCES

1. H. Maeda, L. W. Seymour, and Y. Miyamoto. Conjugates of anticancer agents and polymers: advantages of macromolecular therapeutics *in vivo*. *Bioconjug. Chem.* **3**:351–362 (1992).
2. P. A. Vasey, S. B. Kaye, R. Morrison, C. Twelves, P. Wilson, R. Duncan, A. H. Thomson, L. S. Murray, T. E. Hilditch, T. Murray, S. Burtles, D. Fraier, E. Frigerio, and J. Cassidy. Phase I clinical and pharmacokinetics study of PK1 [*N*-(2-hydroxypropyl)methacrylamide copolymer doxorubicin]: first member of a new class of chemotherapeutic agents-drug-polymer conjugates. *Clin. Cancer Res.* **5**:83–94 (1999).
3. V. R. Ciaolfa, M. Zamai, A. Fiorino, E. Frigerio, C. Pellizzoni, R. d'Argy, A. Ghiglieri, M. G. Castelli, M. Farao, M. Pesenti, F. Gigli, F. Angelucci, and A. Suarato. Polymer-bound camptothecin: Initial biodistribution and antitumor activity studies. *J. Control. Release* **65**:105–119 (2000).
4. P. Julyan, L. Seymour, D. Ferry, S. Daryani, C. M. Boivin, J. Doran, M. David, D. Anderson, C. Christodoulou, A. M. Young, S. Hesslewood, and D. J. Kerr. Preliminary clinical study of the distribution of the HPMA copolymers bearing doxorubicin and galactosamine. *J. Control. Release* **57**:281–290 (1999).
5. Z.-R. Lu, P. Kopeckova, and J. Kopecek. Polymerizable Fab' antibody fragments for targeting of anticancer drugs. *Nature Biotech.* **17**:1101–1104 (1999).
6. G. D. Prestwich. Biomaterials from chemically-modified hyaluronan. *Glycoforum* http://glycoforum.gr.jp (2001).
7. R. M. Peterson, Q. Yu, I. Stamenkovic, and B. P. Toole. Pertur-

bation of hyaluronan interactions by soluble CD44 inhibits growth of murine mammary carcinoma cells in ascites. *Amer. J. Pathol.* **156**:2159–2167 (2000).
8. C. X. Zeng, B. P. Toole, S. D. Kinney, J. W. Kuo, and I. Stamenkovic. Inhibition of tumor growth *in vivo* by hyaluronan oligomers. *Int. J. Cancer* **77**:396–401 (1998).
9. V. B. Lokeshwar, C. Obek, H. T. Pham, D. Wei, M. J. Young, R. C. Duncan, M. S. Soloway, and N. L. Block. Urinary hyaluronic acid and hyaluronidase: Markers for bladder cancer detection and evaluation of grade. *J. Urol.* **163**:348–356 (2000).
10. W. Knudson. Tumor-associated hyaluronan: providing an extracellular matrix that facilitates invasion. *Am. J. Pathol.* **148**:1721–1726 (1996).
11. L. Y. W. Bourguignon, H. B. Zhu, L. J. Shao, and Y. W. Chen. CD44 interaction with Tiam1 promotes Rac1 signaling and hyaluronic acid-mediated breast tumor cell migration. *J. Biol. Chem.* **275**:1829–1838 (2000).
12. J. B. Catterall, L. M. H. Jones, and G. A. Turner. Membrane protein glycosylation and CD44 content in the adhesion of human ovarian cancer cells to hyaluronan. *Clin. Exp. Metastas.* **17**: 583–591 (1999).
13. Y. Yamada, N. Itano, H. Narimatsu, T. Kudo, S. Hirohashi, A. Ochiai, A. Niimi, M. Ueda, and K. Kimata. Receptor for hyaluronan-mediated motility and CD44 expressions in colon cancer assessed by quantitative analysis using real—time reverse transcriptase-polymerase chain reaction. *Jpn. J. Cancer Res.* **90**:987–992 (1999).
14. Y. Matsubara, S. Katoh, H. Taniguchi, M. Oka, J. Kadota, and S. Kohno. Expression of CD44 variants in lung cancer and its relationship to hyaluronan binding. *J. Int. Med. Res.* **28**:78–90 (2000).
15. H. Li, L. Guo, J. W. Li, N. Liu, R. Qi, and J. Liu. Expression of hyaluronan receptors CD44 and RHAMM in stomach cancers: Relevance with tumor progression. *Int. J. Oncol.* **17**:927–932 (2000).
16. A. Yokota, G. Ishii, Y. Sugaya, M. Nishimura, Y. Saito, and K. Harigaya. Potential use of serum CD44 as an indicator of tumor progression in acute leukemia. *Hematol. Oncol.* **17**:161–168 (1999).
17. M. Culty, M. Shizari, E. W. Thompson, and C. B. Underhill. Binding and degradation of hyaluronan by human breast cancer cell lines expressing different forms of CD44: correlation with invasive potential. *J. Cell. Physiol.* **160**:275–286 (1994).
18. Q. Hua, C. B. Knudson, and W. Knudson. Internalization of hyaluronan by chondrocytes occurs via receptor-mediated endocytosis. *J. Cell Sci.* **106**:365–375 (1993).
19. K. Akima, H. Ito, Y. Iwata, K. Matsuo, N. Watari, M. Yanagi, H. Hagi, K. Oshima, A. Yagita, Y. Atomi, and I. Tatekawa. Evaluation of antitumor activities of hyaluronate binding antitumor drugs: Synthesis, characterization and antitumor activity. *J. Drug Target.* **4**:1–8 (1996).
20. Y. Luo and G. D. Prestwich. Synthesis and selective cytotoxicity of a hyaluronic acid-antitumor bioconjugate. *Bioconjug. Chem.* **10**:755–763 (1999).
21. M. B. Hansen, S. E. Nielsen, and K. Berg. Re-examination and further development of a precise and rapid dye method for measuring cell growth/cell kill. *J. Immunol. Meth.* **119**:203–210 (1989).
22. J. M. Kokoshka, C. M. Ireland, and L. R. Barrows. Cell-based screen for identification of inhibitors of tubulin polymerization. *J. Nat. Prod.* **59**:1179–1182 (1996).
23. L. B. Shih, D. M. Goldenberg, H. Xuan, H. Lu, R. M. Sharkey, and T. C. Hall. Anthracycline Immunoconjugates prepared by a site-specific linkage via an amino-dextran intermediate carrier. *Cancer Res.* **51**:4192–4198 (1991).
24. H. Ogura, S. Nagai, and K. Takeda. A novel reagent (*N*-succinimidyl diphenylphosphate) for synthesis of active ester and peptide. *Tetrahedron Lett.* **21**:1467–1468 (1980).
25. J. Kopecek, P. Rejmanova, J. Strohalm, K. Ulbrich, B. Rihova, V. Chytry, J. B. Lloyd, and R. Duncan. Synthetic polymeric drugs. *U.S. Patent 5,037,883 (August 6, 1991)*.
26. V. G. Omelyanenko, P. Kopeckova, C. Gentry, J.-G. Shiah, and J. Kopecek. HPMA copolymer-anticancer drug-OV-TL16 antibody conjugates. 1. Influence of the methods of synthesis on the binding affinity to OVCAR-3 ovarian carcinoma cells in vitro. *J. Drug Target.* **3**:357–373 (1996).
27. D. Puttnam and J. Kopecek. Polymer conjugates with anticancer activity. *Adv. Polym. Sci.* **122**:55–123 (1995).
28. P. Rejmanova, J. Labsky, and J. Kopecek. Aminolyses of monomeric and polymeric p-nitrophenyl esters of methacryloylated amino acids. *Makromol. Chem.* **178**:2159–2168 (1977).
29. Y. Luo, M. R. Ziebell, and G. D. Prestwich. A hyaluronic acid-taxol antitumor bioconjugate targeted to cancer cells. *Biomacromolecules* **1**:208–218 (2000).
30. B. Rihova, P. Kopeckova, J. Strohalm, P. Rossmann, V. Vetvicka, and J. Kopecek. Antibody directed affinity therapy applied to the immune system: *in vivo* effectiveness and limited toxicity of daunomycin conjugates to HPMA copolymers and targeting antibody. *Clin. Immunol. Immunopathol.* **46**:100–114 (1988).
31. J. Kopecek, P. Kopeckova, T. Minko, and Z. R. Lu. HPMA copolymer-anticancer drug conjugates: design, activity, and mechanism of action. *Eur. J. Pharm. Biopharm.* **50**:61–81 (2000).